Compositional pore-network modeling of gas flooding in gas-condensate reservoirs

Paula K. P. Reis[1], Marcio S. Carvalho[1]

[1]*Dept. of Mechanical Engineering, Pontifícia Universidade Católica do Rio de Janeiro*
Rua Marques de São Vicente, 225. 22451-900, Rio de Janeiro, Brazil
paulareis@lmmp.mec.puc-rio.br, msc@lmmp.mec.puc-rio.br

Abstract. Gas flooding in gas-condensate reservoirs can delay pressure depletion below the dew-point and re-vaporize accumulated condensate in the near wellbore region. For condensate bank removal, the method's success depends on a series of parameters, such as the injected gas composition, the total injected volume, the reservoir depletion level and the porous medium heterogeneity. In order to investigate the influence of these parameters at the pore-scale, we used a compositional pore-network model to reproduce gas injection in porous media after condensate accumulation. With the model, the effects of complex phase behavior arisen from the interaction between injected gas and accumulated fluids in the porous medium could be evaluated. The performances of methane, ethane, carbon dioxide, nitrogen and produced gas flooding to improve flow following condensate banking at different pressure levels were compared. Condensate re-vaporization rate, recovery of heavy components, relative permeabilities, and final saturations were quantified so that optimal injection scenarios were identified. Results indicated that the injected gas composition affects significantly condensate banking removal by gas flooding, with C_2 and CO_2 being the most favorable candidates among the tested gases for the method. The injection pressure also affected greatly the results, curtailing the condensate recovery as it was decreased below the dew point.

Keywords: Gas flooding, Pore-network modeling, Gas-condensate reservoirs

1 Introduction

Production from gas-condensate reservoirs can be significantly affected by condensate banking. As the pressure around producing wells is lowered below the reservoir mixture's dew point, a liquid phase emerges in the porous medium and partially blocks the gas flow. Several aspects affect the severity of the damage, such as the reservoir permeability, reservoir fluid composition and depletion level. Even lean gas mixtures can lead to significant flow blockage once liquid dropout takes place [1]. The liquid and gas phases different mobilities and molar contents induce a compositional shift in the two-phase region, which enlarges the local heavier component fractions and can lead to substantial liquid saturations [2].

In order to manage this production challenge, various production strategies and EOR methods have been devised for gas-condensate reservoirs development [3]. Among these methods, many involve the injection of gas in the reservoir, aiming full or partial pressure maintenance, as well as re-evaporation of accumulated condensate.

In full pressure maintenance, the reservoir pressure is kept above the dew point pressure and liquid dropout is prevented. If feasible, this method can maximize condensate recovery, as no liquid phase is deposited in the porous medium and heavy components are produced in the gas. Implementing a full pressure maintenance scheme, however, requires large amounts of injected gas and can be unpractical for cases in which the initial reservoir pressure is close to the fluids dew point [4]. Also, special attention has to be directed to the injected gas composition. Certain gases, such as N_2 [4] and C_1 [5], have a tendency to increase gas-condensate mixtures dew point and can lead to early condensation in the reservoir.

For the case of partial pressure maintenance, gas can be injected following liquid dropout in the reservoir. In this approach, the objectives are both slowing down pressure depletion and re-vaporizing the accumulated condensate, so that gas flowing paths are cleared and valuable heavy components are recovered. Flooding experiments using C_1 [6–8], N_2 [6], CO_2 [6, 7, 9] and lean gas [6, 10] in condensate rich cores demonstrate the method's ability to improve flow and indicate a significant influence of the injected gas composition in liquid banking removal. Additionally to core flooding tests, several reservoir-scale numerical studies have been conducted to assess gas injection as an enhanced gas-condensate recovery method. In these studies, a series of parameters affecting flow enhancement via gas-flooding, such as the time for injection [11], the injected gas composition [12–15] and the presence of fractures in the reservoir [14, 15] have been evaluated. Overall, CO_2 and C_2 displayed greater potential to re-vaporize condensate, when compared to C_1, N_2 and lean gas, although contradicting results [12] have been found. Moreover, most studies indicated that condensate recovery increased considerably with injection pressure.

Although both experimental and numerical studies indicate that gas injection is an advantageous approach for condensate enhanced recovery, no pore-scale analysis of the method have been reported in the literature. This leads to a significant lack in data for gas injection performance evaluation, especially considering that pore-scale events are essential to understanding macro-scale transport properties in porous media. During gas injection, local changes in composition can alter significantly both bulk and interfacial properties of gas and liquid phases, which in turn affect their flow characterized by the relative permeability curves. To address this gap, we used a compositional pore-network model to evaluate gas injection in porous media after condensate accumulation. The model had been validated against core flooding experiments [16] and also used to evaluate wettability alteration as a gas-condensate enhanced recovery method [17]. In the present study, first we replicated condensate accumulation in the porous medium by flowing a representative gas-condensate mixture through a sandstone-based network at different depletion levels, starting from values just below the dew point, until pressures below the maximum liquid dropout. Then C_1, C_2, CO_2, N_2 or produced gas were injected in the condensate bearing networks and the flow improvement was evaluated. Final saturations, relative permeabilities and recovery of heavy hydrocarbon components were quantified to compare the efficacy of each injection scenario.

2 Pore-network model

The pore-network model used in the present study was devised specifically to represent gas-condensate flow in porous media. It was based on the fully compositional pore-network model proposed by Santos and Carvalho [18] and adapted to encompass realistic characteristics of *in-situ* condensate formation and gas-condensate flow. The model is presented in detail by Reis and Carvalho [16].

2.1 Governing Equations

A system of non-linear equations relates the molar content and pressure of each pore in the networks representing porous media. It encompasses molar balance equations (eq. (1)) and volume consistency equations (eq. (2)).

The molar balance equations describe how the number of moles in a pore volume i vary due to the molar flow rate through its adjacent pore throats, $\dot{n}_j^k$, and the flow at the network boundaries, $\dot{s}_i^k$. In this equation, c_{ij} are the entries of the incidence matrix C, which maps which throats are connected to each pore volume in the network. The molar flow through a pore throat, given by eq. (1)b, converts the volumetric flow, calculated with the conductances g and the pressure drop ΔP, into the molar flow, using the molar fraction of each component in the gas and liquid phases, y^k and x^k, and their molar densities, ξ_g ans ξ_l. Equation 1c represents the pressure that drives the flow through the throats. The inclusion of the interface pressure difference (ΔP_j^{int}) in eq. (1)c is controlled by the parameter H^{int}, which indicates the presence of fluid meniscii in the throats. In eq. (1), $i = 1..n_b$, $j = 1..n_t$, and $k = 1..n_c$, represent, respectively, the number of pore volumes, pore throats and fluid mixture components in a network.

$$\frac{\partial N_i^k}{\partial t} = -\sum_{j=1}^{n_t} c_{ij}\dot{n}_j^k + \dot{s}_i^k \tag{1a}$$

$$\dot{n}_j^k = (y^k \xi_g g_g + x^k \xi_l g_l)_j \Delta P_j \tag{1b}$$

$$\Delta P_j = \sum_{m=1}^{n_b} c_{mj} P_m - H_j^{int} \Delta P_j^{int} \tag{1c}$$

The volume consistency equations, given by eq. (2), are used to enforce compatibility between the pore volumes and the volumes of the phases contained in them. These equations are devised considering slightly compressible networks, so that, for a given pressure P_i, the volume of a pore can be approximated using the pore compressibility, ν_i, along with reference volume, $\overline{V_i}$, and pressure, $\overline{P_i}$ values. For the calculation of the gas and liquid phases volumes, the pressure and temperature in the pore, P_i and T, are related with the fluid parameters $\mathcal{L}_i$, Z_i^g, Z_i^l, x_i^k and y_i^k (respectively: the fraction of the N_i moles in the liquid phase, the compressibility factors and the molar fractions of each component k in the gas and liquid phases).

$$N_i - \frac{\overline{V_i}[1 + \overline{\nu_i}(P_i - \overline{P})]}{\mathcal{L}_i\left(\frac{Z_i^l RT}{P_i} - \sum_{k=1}^{n_c} v_k x_i^k\right) + (1 - \mathcal{L}_i)\left(\frac{Z_i^g RT}{P_i} - \sum_{k=1}^{n_c} v_k y_i^k\right)} = 0 \tag{2}$$

Additionally to eq. (1) and eq. (2), simple equations are written to enforce the boundary conditions for the system. In the presented model, the flow can be driven either by imposing different pressure levels at the inlet and the outlet, or by prescribing molar flow rate at the inlet and pressure at the outlet. Other parameters that have to be imposed are the composition of the fluid injected in the network and the temperature T.

The presented system of equations was based on the compositional formulation proposed by Collins et al. [19], which decouples the flow equations from the flash calculations. In this formulation, the system relating flow equations is solved with the Newton-Raphson method, while thermodynamic equilibrium is enforced at each newton iteration, by performing phase equilibrium calculations with the Peng-Robinson EoS using the trial solution variables. Details of the implemented phase equilibrium calculations can be found in Santos and Carvalho [18].

3 Outline of the presented analyses

3.1 Pore-network

The pore-network used in the present study represented a $1.75mm^3$ cubic section of a sandstone with permeability of $169mD$ and porosity of 17.1%. This network was first extracted from Micro-CT imaging of a sandstone sample, using the network extraction algorithm proposed by Dong [20], then adapted to meet the geometric criteria described in Reis and Carvalho [16], which involves the use of converging-diverging pores. Figure 1a illustrates the pore-network topography, Fig. 1b the size distribution of the unconstricted radius of the pores (R_{max}), and Fig. 1c the size distribution of the constricted radius of the pores (R_{min}). More details of the network adaptation process can be found in Reis and Carvalho [17].

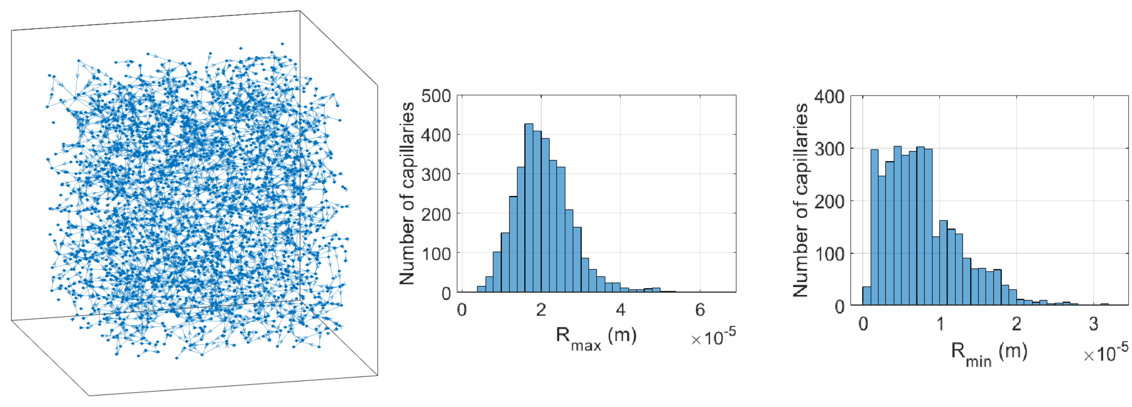

(a) Topography of the pore-network adapted from Dong [20]

(b) Distribution of R_{max} in the used pore-network

(c) Distribution of R_{max} in the used pore-network

Figure 1. Pore-network representing a sandstone with $K = 169mD$ ans $\phi = 17.1\%$

3.2 Fluids

The composition of the fluid used during the condensate accumulation process in the porous medium is presented in Table 1. This mixture represents a typical fluid found in gas-condensate reservoirs, composed by carbon dioxide, nitrogen, light, intermediate and heavy hydrocarbons. It exhibits a large window of retrograde condensation behavior in the temperature range from $12°C$ to $207°C$, as shown in the phase diagram in Fig. 2. For our analyses, a temperature of $60°C$ was chosen as the reservoir temperature.

Besides produced gas, C_1, C_2, CO_2 and N_2 were chosen as the candidates for condensate enhanced recovery. For the sake of appraising preliminarily the ability of these gases to re-vaporize condensate, Fig. 3 illustrates the

Table 1. Gas-condensate mixture composition

Component	Molar Fraction
CO_2	0.05
N_2	0.02
C_1	0.65
C_2	0.13
C_3	0.07
C_6	0.05
C_{10}	0.025
C_{16}	0.005

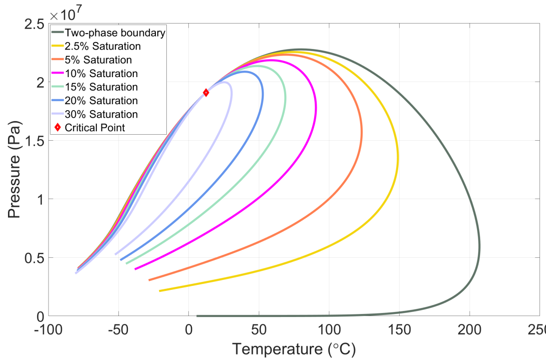

Figure 2. Fluid mixture phase envelope

liquid dropout as a function of pressure obtained by mixing C_1, C_2, CO_2 or N_2 with the composition presented in Table 1, at different molar fractions and a temperature of $60°C$.

It can be noticed from Fig. 3 that increasing the content of C_1, C_2, CO_2 or N_2 in the representative reservoir fluid mixture leads to a progressive reduction in the liquid saturation. This result suggests that the tested gases have a positive prospect to work as condensate re-vaporization agents and, consequently, improve gas flow in porous media. It should be remarked, however, that mixing both C_1 and N_2 with the reservoir mixture also led to an increase in the dew point pressure. Therefore, while reducing the maximum liquid dropout, these gases can promote an early condensation and might cause negative effects on flow, if injected at high pressures.

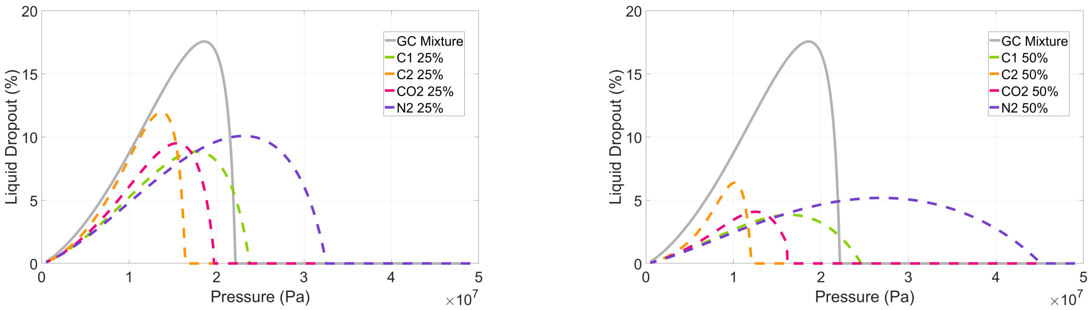

(a) 75% of the gas-condensate mixture and 25% of the injected gases

(b) 50% of the gas-condensate mixture and 50% of the injected gases

Figure 3. Liquid dropout at a temperature of $60°C$

3.3 Flow conditions

Two steps of injection were performed in the network for every evaluated case. First, 25 pore volumes of the reservoir fluid were injected so that condensate accumulated in the porous medium, mimicking the process of condensate banking in the near wellbore regions. Then, the injected composition in the network was altered, so that the liquid buildup was followed by condensate recovery during the injection of 25 pore volumes of the tested gases.

These injection steps were repeated at different pressures. As the timing for gas injection is one of the most relevant parameters for the method's success [11], we wanted to test its performance at various reservoir depletion stages. Six pressure values were used, 22, 21.5, 21, 19.5, 17.75 and 14.75 MPa, which corresponded to liquid dropout saturations of 2.3%, 9.7%, 13.3%, 17.1%, 17.3% and 14.7%, respectively. With that, a broad range of depletion scenarios could be covered, from the early stages of condensate formation to pressures below the maximum liquid dropout.

The prescribed boundary conditions for both steps were molar flow rate at the network inlet and pressure at the outlet. For all tested injection scenarios, the molar flow rate was adjusted so that a gas flowing velocity of $35m/day$ was achieved. It has been reported in the literature [6] that injection rate does not influence significantly the performance of gas injection as a gas-condensate EOR method and we chose, therefore, not to explore the effects of this parameter.

4 Results

4.1 Condensate saturation reduction

Figures 4(a)-(d) illustrate the evolution of the condensate saturation in the network with time. These curves represent both the condensate buildup during the injection of the reservoir fluids and the condensate recovery during gas injection. At the pressure of $22 MPa$, just below the dew point pressure, C_2 and CO_2 produce almost identical effects on the accumulated condensate. Both reduced the liquid content faster and to a lower saturation than the other tested gases. C_1 also reduced significantly the condensate saturation, while N_2 and produced gas displayed the lowest capacity to recover condensate. Similar results were obtained with gas injection at the pressure of $21 MPa$. Even though the amount of accumulated condensate in the networks increased significantly, corresponding to 32.06%, the injected gases cleared the liquid damage efficiently. This is a good indicative that, at high pressures, all tested gases could be used to support reservoir pressure and recover the accumulated liquid. As the injection pressure is lowered below $20 MPa$, however, the ability of the gases to recover condensate is clearly reduced, as shown in Fig. 4(c) and (d). The rate of liquid re-vaporization is progressively slowed down during the injection of all tested gases, indicating that more injected volume is required for the same volume of recovered condensate, as the reservoir becomes more depleted. At the lowest tested pressure, $P = 14.75 MPa$, all tested gases perform similarly, leaving most of the condensate in the porous medium after the injection of 25 PV. These findings support the hypothesis that the timing for injection of gases in gas-condensate reservoirs is crucial for effective condensate recovery and gas flow improvement.

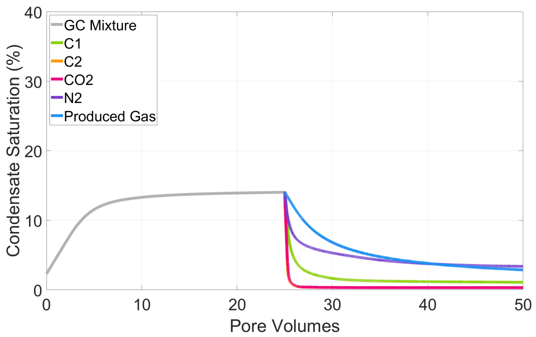

(a) $P = 22 MPa$

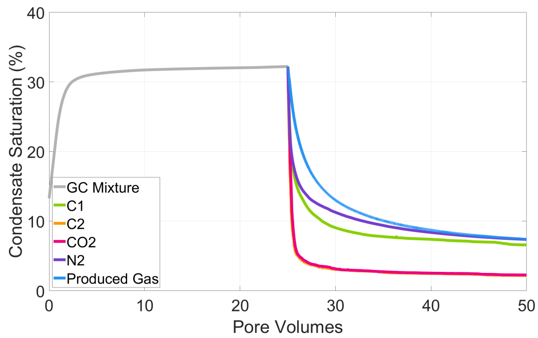

(b) $P = 21 MPa$

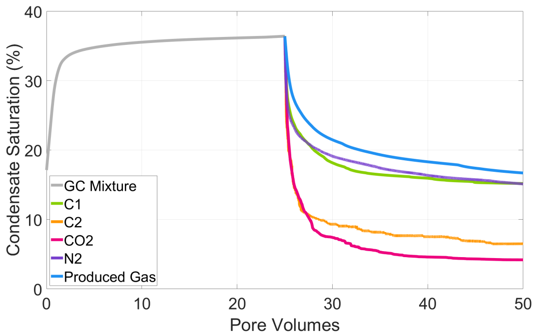

(c) $P = 19.5 MPa$

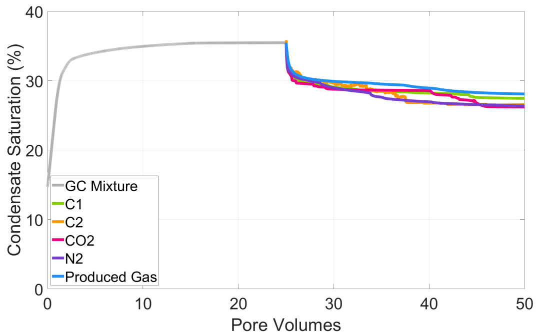

(d) $P = 14.75 MPa$

Figure 4. Condensate saturation evolution with time in the networks.

4.2 Recovery of heavy components

Ideally, a gas mixture injected in a gas-condensate reservoir should be able to re-vaporize not only light, but also medium and heavy components accumulated in the porous medium during condensate banking. For this reason, the recoveries of the three heaviest components of the gas-condensate fluid used in this study, namely hexane, C_6, decane, C_{10} and hexadecane, C_{16}, were quantified during all tested gas injection scenarios and are presented in Fig. 5.

The results in Fig. 5 suggest that C_1, C_2 and CO_2 are able to recover the three heaviest components evenly. For these cases, the recoveries of each analyzed component can be directly related to the reduction in liquid

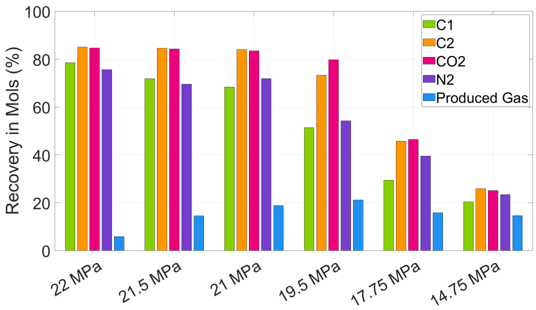

(a) C_6 Recovery

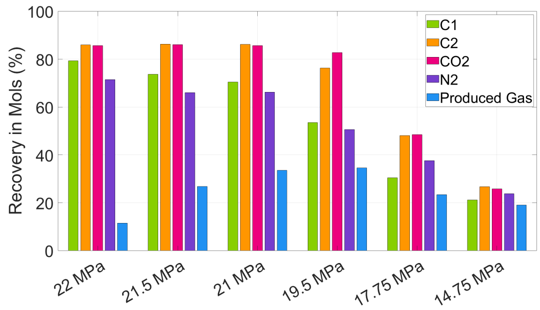

(b) C_{10} Recovery

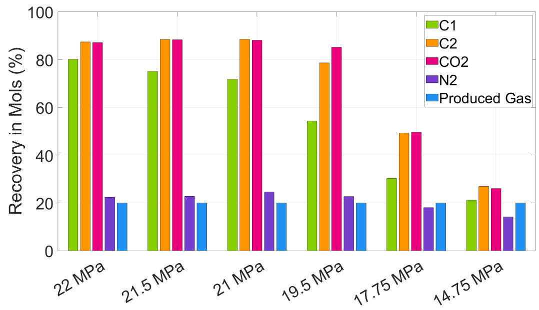

(c) C_{16} Recovery

Figure 5. Recovery per mixture component.

saturation shown in Fig. 4. During the injection of N_2, however, the recovery of hexadecane was considerably lower than the recoveries of hexane and decane. Therefore, in this case, during the re-vaporization of condensate, the remaining liquid in the porous medium becomes particularly rich in C_{16}, impeding its recovery. This indicates that nitrogen may be unable to retrieve the heaviest components accumulated in gas-condensate reservoirs. As for the injection of the produced gas, the recoveries of the three heaviest components were significantly lower than those obtained during the injection of the other tested gases.

4.3 Gas Relative Permeability

As a way of directly quantifying the gas flow improvement with gas injection, in this section, we compared the gas relative permeabilities (k_{rg}) before and after the treatment. Figure 6 presents these results for all tested pressures. The data in grey represents the k_{rg} after the injection of 25 pore volumes of the reservoir mixture, while the other colors represent the k_{rg} following the injection of 25 pore volumes of C_1, C_2, CO_2, N_2 or produced gas. For pressures above $20MPa$, the injection of all tested gases could restore the k_{rg} to values above 0.8, indicating a significant flow improvement. For $P = 19.5MPa$, flooding the porous medium with C_2 or CO_2 could still recover the gas permeability almost completely, while the other tested gases led to $k_{rg} \approx 0.6$. At $P = 17.75MPa$, significant differences could also be found between the k_{rg} values achieved following C_2 or CO_2 injection from those obtained with CO_2, N_2 or produced gas. Finally, at the lowest tested pressure, all injection scenarios produced gas relative permeabilities below 0.4.

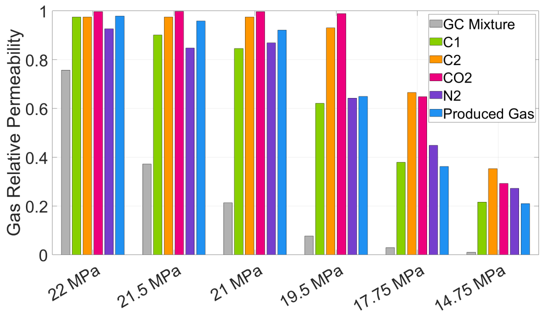

Figure 6. Gas relative permeabilities before and after gas injection.

5 Conclusions

The present study provided a pore-scale evaluation of gas injection as a condensate enhanced recovery method. By using a compositional pore-network model, the effects of injected composition and pressure could be investigated by quantifying liquid saturation reduction, heavy component recovery and the impact on gas relative permeabilities. With these criteria, the performances of injecting C_1, C_2, CO_2, N_2 and produced gas to recover the condensate accumulated in a sandstone based pore-network at different depletion stages were compared, without the presence of connate water .

The results indicated that gas injection can produce substantial flow improvement in damaged gas-condensate reservoirs, given that the injected gas composition and pressure for the treatment are adequately determined. Injecting C_2 and CO_2 generated the most favorable results among the tested gases, followed by C_1, produced gas and N_2.

As a preliminary investigation of gas injection in gas-condensate reservoirs at the pore-scale, this work exposed how the injection pressure and the gas composition can impact significantly the two-phase flow during condensate recovery and, consequently, the method's efficiency. As future work, a systematic pore-scale investigation of the parameters affecting condensate recovery with gas injection, as flow rate, gas-condensate fluid composition and porous media heterogeneity should be carried out. With that, data for up-scaling pore-scale effects pertaining to particular gas injection scenarios could be generated for reservoir-scale modeling. This could lead to more realistic recovery estimations and benefit gas-condensate fields development planning.

Acknowledgements. This research was funded by Repsol-Sinopec Brasil, under the RD&I Levy Fund Program of the National Petroleum Agency (ANP).

Authorship statement. The authors hereby confirm that they are the sole liable persons responsible for the authorship of this work, and that all material that has been herein included as part of the present paper is either the property (and authorship) of the authors, or has the permission of the owners to be included here.

References

[1] D. Afidick, N. Kaczorowski, S. Bette, and others. Production performance of a retrograde gas reservoir: a case study of the arun field. In *SPE Asia pacific oil and gas conference*. Society of Petroleum Engineers, 1994.

[2] H. X. Vo, R. N. Horne, and others. Experimental study of composition variation during flow of gas-condensate. In *SPE Annual Technical Conference and Exhibition*. Society of Petroleum Engineers, 2015.

[3] A. Hassan, M. Mahmoud, A. Al-Majed, M. B. Alawi, S. Elkatatny, M. BaTaweel, and A. Al-Nakhli. Gas condensate treatment: A critical review of materials, methods, field applications, and new solutions. *Journal of Petroleum Science and Engineering*, vol. 177, pp. 602–613, 2019.

[4] K. Luo, S. Li, X. Zheng, G. Chen, Z. Dai, N. Liu, and others. Experimental investigation into revaporization of retrograde condensate by lean gas injection. In *SPE Asia Pacific Oil and Gas Conference and Exhibition*. Society of Petroleum Engineers, 2001.

[5] T. Ahmed, J. Evans, R. Kwan, T. Vivian, and others. Wellbore liquid blockage in gas-condensate reservoirs. In *SPE eastern regional meeting*. Society of Petroleum Engineers, 1998.

[6] H. A. Al-Anazi, M. M. Sharma, G. A. Pope, and others. Revaporization of condensate with methane flood. In *SPE Annual Technical Conference and Exhibition*. Society of Petroleum Engineers, 2004.

[7] A. Al-Abri, H. Sidiq, and R. Amin. Mobility ratio, relative permeability and sweep efficiency of supercritical co2 and methane injection to enhance natural gas and condensate recovery: Coreflooding experimentation. *Journal of Natural Gas Science and Engineering*, vol. 9, pp. 166–171, 2012.

[8] S. Sharma, J. J. Sheng, and Z. Shen. A comparative experimental study of huff-n-puff gas injection and surfactant treatment in shale gas-condensate cores. *Energy & fuels*, vol. 32, n. 9, pp. 9121–9131, 2018.

[9] X. Meng, Z. Meng, J. Ma, T. Wang, and others. Performance evaluation of co 2 huff-n-puff gas injection in shale gas condensate reservoirs. *Energies*, vol. 12, n. 1, pp. 1–18, 2018.

[10] X. Meng, J. J. Sheng, and others. Experimental study on revaporization mechanism of huff-n-puff gas injection to enhance condensate recovery in shale gas condensate reservoirs. In *SPE improved oil recovery conference*. Society of Petroleum Engineers, 2016.

[11] D. Marokane, A. Logmo-Ngog, R. Sarkar, and others. Applicability of timely gas injection in gas condensate fields to improve well productivity. In *SPE/DOE Improved Oil Recovery Symposium*. Society of Petroleum Engineers, 2002.

[12] J. T. Linderman, F. S. Al-Jenaibi, S. G. Ghori, K. Putney, J. Lawrence, M. Gallat, K. Hohensee, and others. Feasibility study of substituting nitrogen for hydrocarbon in a gas recycle condensate reservoir. In *Abu Dhabi International Petroleum Exhibition and Conference*. Society of Petroleum Engineers, 2008.

[13] A. Zhang, Z. Fan, and L. Zhao. An investigation on phase behaviors and displacement mechanisms of gas injection in gas condensate reservoir. *Fuel*, vol. 268, pp. 117373, 2020.

[14] A. Taheri, L. Hoier, O. Torsaeter, and others. Miscible and immiscible gas injection for enhancing of condensate recovery in fractured gas condensate reservoirs. In *EAGE Annual Conference & Exhibition incorporating SPE Europec*. Society of Petroleum Engineers, 2013.

[15] A. H. Fath, A.-R. Pouranfard, R. Parandvar, and S. Pourhadi. An investigation of different gas injection scenarios as enhanced condensate recovery method in a naturally fractured gas-condensate reservoir. *Petroleum Science and Technology*, vol. 34, n. 3, pp. 295–301, 2016.

[16] P. Reis and M. Carvalho. Pore-scale compositional modeling of gas-condensate flow: Effects of interfacial tension and flow velocity on relative permeability. *Journal of Petroleum Science and Engineering*, vol. , pp. 108454, 2021.

[17] P. K. Reis and M. S. Carvalho. Pore-scale analysis of condensate blockage mitigation by wettability alteration. *Energies*, vol. 13, n. 18, pp. 4673, 2020.

[18] M. Santos and M. Carvalho. Pore network model for retrograde gas flow in porous media. *Journal of Petroleum Science and Engineering*, vol. 185, pp. 106635, 2020.

[19] D. Collins, L. Nghiem, Y. Li, J. Grabonstotter, and others. An efficient approach to adaptive-implicit compositional simulation with an equation of state. *SPE reservoir engineering*, vol. 7, n. 02, pp. 259–264, 1992.

[20] H. Dong. *Micro-CT imaging and pore network extraction*. PhD thesis, Department of Earth Science and Engineering, Imperial College London, 2008.